ISSN 2347 - 3983
Volume 8. No. 10, October 2020
International Journal of Emerging Trends in Engineering Research
Available Online at http://www.warse.org/IJETER/static/pdf/file/ijeter1568102020.pdf
https://doi.org/10.30534/ijeter/2020/1568102020

Post-Bonding Application for Vehicle Antiroll Bars' Rubber-Metal Bushes

Gulnara K.Taimanova[1], AigulK.Kozhakhan[2], BakhytkulU.Baikhozhaeva[3], AbdullaU.Akhmedyanov[4], KamilyaZ.Kirgizbayeva[5]

[1]PhD in Technical Sciences, Associate Professor, L.N.Gumilyov Eurasian National University, The Faculty of Transport and Energy, Department of Standardization, certification and metrology, Nur-Sultan, Republic of Kazakhstan, gtaimanova@mail.ru
[2]PhD in Technical Sciences, Acting Professor, Al-Farabi Kazakh National University, Department Geography and Environmental Sciences, UNESCO Chair in sustainable development,Almaty, Republic of Kazakhstan, aigul_k@mail.ru
[3]Doctor of Technical Sciences, Professor,L.N.Gumilyov Eurasian National University, Department of Standardization, certification and metrology, Nur-Sultan, Republic of Kazakhstan, Bajxozhaeva63@mail.ru
[4]PhD in Technical Sciences, L.N.Gumilyov Eurasian National University, The Faculty of Transport and Energy, Department of Standardization, certification and metrology, Nur-Sultan, Republic of Kazakhstan, abdulla@yandexl.ru
[5]PhD in Technical Sciences, Associate Professor,L.N.Gumilyov Eurasian National University, The Faculty of Transport and Energy, Department of Standardization, certification and metrology, Nur-Sultan, Republic of Kazakhstan, Kirg_kam@mail.ru

ABSTRACT

In this presented study, major production parameters of the Post-Bonding method are changed systematically. Their effects on bonding strength are investigated and optimized experimentally. Using vulcanization as an example, it has been experimentally shown that the new post-bonding technology works as a production process. In study showed that the technique of subsequent bonding improves the quality and service life of parts in systems of antiroll bars. A new post-bonding application for adhesion of the rubber-metal parts was developed. The parameters of this technique were investigated and applied to rubber-metal couple adhesion of the automobile antiroll bar's bushes as a practical application Mechanical requirements of the rubber bushes were determined. adial stiffness measurements and tensile tests were performed to verify the optimized designs. The results were compared to evaluate outputs of the new post-bonding technique. As a result, the interactions of the parameters have been investigated to each other and better cases are selected. The technique was reduced to molding process in the long anti roll bar and rubber bushes to combining needs.

Keywords: adhesion, compression ratio, post-bonding technique, vehicle antiroll, vulcanization.

1. INTRODUCTION

In a wide range of anti-vibration applications, rubber is designed with the support of metal, aluminum and plastic rigid substrates to make components suitable for assembly and long service life. Bonding the materials to each other takes first place between these methods [1],[2].

In classical bonding applications of rubber assemblies, engineering materials are being bonded together under compression inside the mold during vulcanizing raw rubber onto a metallic surface coated with an adhesive reactive bonding layer. In this stage raw rubber gets elastic properties and materials are bonded together as requested [3].

Various studies are performed on vulcanization bonding process for the manufacturing of rubber-to-metal bonded parts to reduce noise and vibrations of vehicles [4].In vulcanization bonding process, rubber metal parts have to be put in a vulcanization mold tool sizing the largest dimension of the parts which usually requires a big-sized mold with high costs [5].

In this study, a new bonding method is developed and the relations of production parameters to each other are investigated. "Passenger vehicle antiroll bar" is chosen as a case study to make a detailed investigation on an industrial area. During this assembly, a pre-compression is applied on rubber-metal bushes that provides a relative connection between rubber-metal bush and antiroll bar. The expectation from complete antiroll bar system is to help vehicle handling behavior and also to isolate the vibration which comes from road to vehicle body. The parts, which are being produced with this new post-bonding method, have to give equal or better mechanical performance than the conventionally produced ones.

Additionally, this method helps to improve the product quality and comfort conditions to reduce designing time of parts and the amount of design constraints. This is particularly important within recent demand for increasing vehicle safety control using new technologies (e.g. GPS [6]and neural networks [7]), and experimental evaluation of the quality of the materials used in vehicle parts [8].

The mentioned method is called as "Post-Bonding". In this production method, rubber bush and assembly brackets are produced separately same as the conventional production method. Synthetic bonding agents are applied on bonding area between semi-cured rubber bushes and antiroll bar. Rubber-metal bushes are fixed on antiroll bar with assembly brackets. The complete product goes into ovens of which temperature and time parameters are defined to finish the vulcanization. In this presented study, major production parameters of the Post-Bonding method are changed systematically. Their effects on bonding strength are investigated and optimized experimentally.

2. MATERIALS AND METHODS

2.1 Antiroll Bar System

Antiroll bar systems help vehicle handling performance. Antiroll bars are connected to vehicle wheels at the end of bars and from the middle area to the vehicle body [9], [10]. This connection creates a way for vibration which comes from road to vehicle body [11], [12]. To isolate this vibration, rubber bushes are used between antiroll bar and vehicle body [13]**.** These mechanical requirements are defined as radial stiffness (N/mm), axial stiffness (N/mm) and torsional stiffness (Nm/°).

Bushes of antiroll bars are designed under the limitation of the current manufacturing techniques and assembly methods to obtain comfort conditions driving quality and mechanical properties.

During vehicle life, bushes of antiroll bar and inner surface of rubber bushes can be worn out, so an unexpected high amount of tire loads on antiroll bar which causes a relative motion between antiroll bar and bushes. As a result, the antiroll bar rotates inside the bushes. The relative rotation of the bars inside the bushes can be reduced by different design and production techniques [14]. One of them is an additional compression process to bushes during assembling with the bar. But, due to this, the residual stresses on the bushes increase [15],[16],[17]. This causes a reduction in life of the rubber materials of which root case is increased by internal heat [18]. Other techniques are to design internal bush geometry by narrowing and flattening two lateral inner hole sides[19],[20]. This new design produces more geometrical contact to obtain torques by the same shape of the bars. The undesired residual stresses still exist in these bushes [21],[22].

In the parts, the assembly places were fixed for each design and diameter of the assembly hole was taken as Ø40 mm (Figure 1).

The expected mechanical properties of the described bush designs were the same. They were designed in two different geometrical types due to different application techniques.

Short steel bars were covered with antistatic paints and used as antiroll bars.

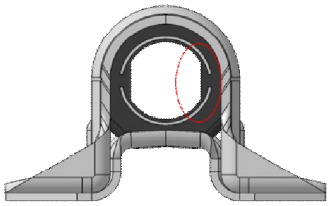

Figure 1: Internal Geometry of Antiroll Bar Bush

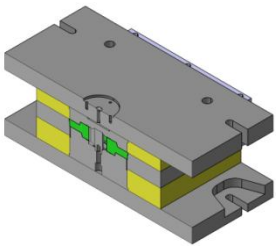

Figure 2: Vulcanization Mold Isometric View

2.2 Experimental Specifications and Set-Ups

The produced samples were used in the experiments for verification of the FEA simulations (Figure 2). The experimental setup was given in Figure 3.

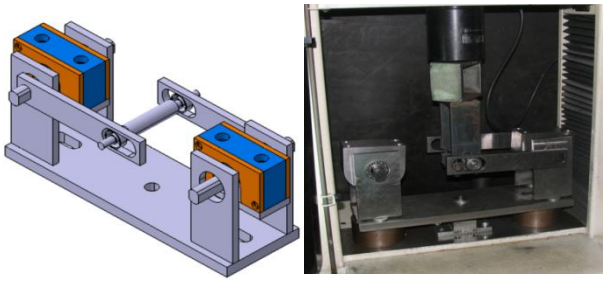

(a) (b)

Figure 3:a) Isometric View of the Designed Experimental Set-Up
b) Produced Experimental Set-Up

The pre-compression fixtures can be seen in Figure 4. Specimens were compressed by fixtures, up to 5% and 10% strain levels. Inner hole sizes of compression molds were Ø39,9 mm and Ø37,8 mm to obtain 5% and 10% pre-compressions levels.

2.3 Finite Element Method (FEM) Simulations

FEM simulations were applied after the description of the geometry, material properties, loads and boundary conditions. The geometry was divided by Finite Elements with optimization of the element number and size.

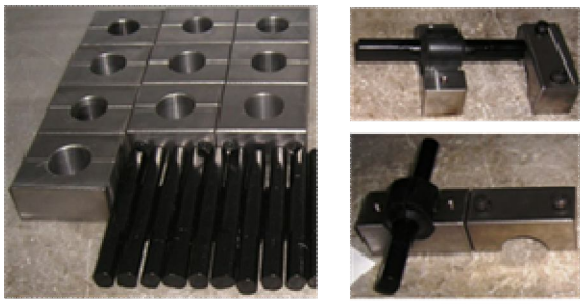

a) b)

Figure 4a) 5% and 10% Compression Molds b) Assembling of the Compression Mold

In FE Analysis, the results directly depend on the described material properties for analysis. Some engineering material properties and characteristics such as steel and aluminum can be found in the literature. The material properties for each compound have to be found by experiments. Compression, tension and shear loaded specimens give the nonlinear hyperelastic material constants [23]. In model parts half geometry was used due to symmetry.

The boundary conditions were simplified by fixing out boundary as the inside, Ø40 mm and radial displacement was applied inside boundary.

2.4 The Post-Bonding Method

In the post-bonding method, antiroll bar rubber-based bushes were semi-vulcanized in the injection molds firstly. After assembling, second vulcanization process was applied in the temperature and time controlled ovens to complete curing in the rubber and it increased the strength of the rubber-steel bonding by chemically linking.

The antiroll bar and the bushes system were tested to measure the level of the expected performance by using radial rigidity experiments[24].

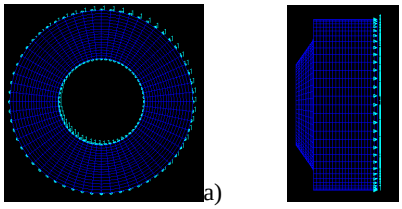

a)

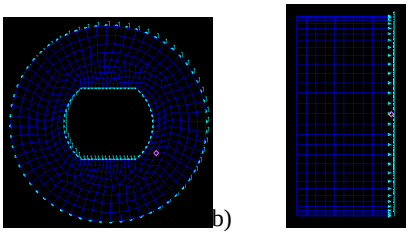

b)

Figure 5: Studied Bushes, FEA Models, Front and Side Views a) Bonded Bushes b) UnbondedFlat Sided Bushes

2.5 Mechanical Properties of the Antiroll bar Bushes and Designing a Comparison System

Two different designs of anti roll bar bushes were developed to understand post-bonding effect on the performance of bushes (Figure 5). The bushes of mechanical performance without bar contact effect were designed as equally. It can be seen in Figure 6, used bush shapes in the post-bonded and unbonded specimen preparation. Unbonded specimen was assembled to the anti roll bar only by compression.

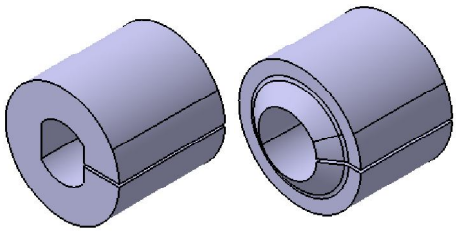

(a) (b)

Figure 6: Designed Bushes a) Compression Type b)Post-Bonded Type

Mechanical performance of the bushes was taken equal according to radial rigidity. The radial rigidity of the designed bushes was selected as 1500 N/mm. It was decided to radial rigidity value with respect to the most used anti roll bar bush properties in the passenger cars. Bush shape geometries were finalized when obtained radial rigidity values as 1500±15% N/mm by using CAD/CAE design and verification loops.

2.6 Application of the Adhesive Agents in the Post-Bonding Process

In the post-bonding process, two layered adhesive chemical agents were used. The first layer (primer) was applied with phenolic resin based and the second layer (seconder) was a special polymer dispersion and other additives. The first layer was applied on the steel surface and the second layer between first layer and rubber surfaces.

The bonding agents are selected with respect to rubber type, hardness and design of the bushes. Bonding agents are two different types; water based and solvent based. In the water based agents, before first and second layer application, the rigid pieces have to be heated around 60°C-80°C.

The rigid parts of the bushes are selected according to bush design requirements, such as rigidity and weight. Generally steel alloys are used. Under convenient conditions almost all engineering materials can bond with rubbers [25].

2.7 Post-Bonding Parameters

The vulcanization process depends on temperature, time and pressure. In the post-bonding process, the parameters, vulcanization ratio and curing time were taken as additional research variables. As a result, the investigated parameters were described as:

a) compression ratio (Stress between surface/Applied Pressure);
b) vulcanization ratio;
c) curing time;
d) curing temperature.

The investigated parameters (Compression Ratio, Vulcanization Ratio, Curing Time and Curing Temperature)were called Factors and their values are named as Levels[26]. Each Factor and Levels were given in Table 1. The response was Bonding Force. The experiments were designed with L16 orthogonal arrays for four Factors and two Levels by using the Taguchi DoE Method. Table 2 shows the experiments needed according to Taguchi DoE Method. Totally 16 experiments were described to observe the influence of the parameters.

Table 1: Factors and Levels

Factor	Parameters	Level 1	Level 2
A	Compression Ratio	5%	10%
B	Vulcanization Ratio	80%	90%
C	Curing time	2 hour	3 hour
D	Curing temperature	170°C	180°C
Response	Bonding Force		

Table 2: Experiments

Experiment	Repeat
5%Compression 80% Vulc. 2 hours at 170 °C	2
5% Compression 80% Vulc. 2 hours at 180 °C	2
5%Compression 90% Vulc. 3 hours at 170 °C	2
5%Compression 90% Vulc. 3 hours at 180 °C	2
10% Compression 80% Vulc. 3 hours at 170 °C	2
10% Compression 80% Vulc. 3 hours at 180 °C	2
10% Compression 90% Vulc. 2 hours at 170 °C	2
10% Compression 90% Vulc. 2 hours at 180 °C	2

2.8 Bonding Experiment

The bonding force measurements were performed by using bonding experiment [27]. The adhesion force between bar and rubber was obtained from the experiments [28].Validity limit in the interface adhesion was required at least 90% rubber fracture without interface fracture or slide. In the bonded specimens, bonding force has to be at least equal or more than only vulcanized type specimens. In Figure 7,onlyexperimental post mortem images of vulcanized type specimens were given. It shows rubber shear fracture. Bonding experiments were performed by using Shimadzu 100kN universal testing machine. The experimental setup can be seen in the Figure 8.

(a) (b)

Figure 7: Postmortem Images of the Vulcanized Specimen after Bonding Experiments

Figure 8: Setup of the Bonding Experiment

3. RESULTS AND DISCUSSION

3.1 Finite Element Analysis Results

Finite Element Analysis was performed to obtain two different shapes but same rigidity bushes convenient for Post-bonding and just vulcanizing respectively.

Table 3: FEA Results after final design loop

Antiroll Bar Bush Type	FEA Result (N/mm)	Deviation (%)	Rubber Hardness (ShA)
Unbonded	1603.77	+6.90	60
Bonded	1498.22	-0.10	55

3.2 Radial Stiffness Experiments

After FEA results, the final designs were produced as specimens according to unbonded and bonded procedures. The results show that both types of the bushes were ensured by the purposed rigidity value within the tolerances. According to these results (Figure 9),post-bonding technique achieves purposed radial rigidity limits as well as production advantages.

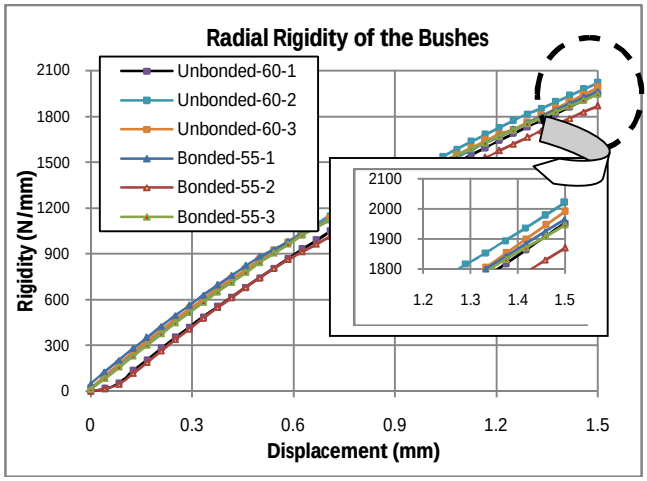

Figure 9: Radial Loading Experimental Results of the Bonded and Unbonded Specimens

Table 4: Radial rigidity experiment results of the bonded specimens

Adhesive Bonded Specimens	FEA	Purposed Value	FEA Deviation
1555.54 N/mm 1642.23 N/mm 1602.77 N/mm Average : 1600.18 N/mm	1603,77 N/mm	1500 N/mm	%6,9

Table 5: Radial rigidity experiment results of the unbonded specimens

Unbonded Specimens	FEA	Purposed Value	FEA Deviation
1584.65 N/mm 1590,10 N/mm 1576.31 N/mm Average: 1583.31 N/mm	1498,22 N/mm	1500 N/mm	%0,12

3.3 Shear Strength of Unbonded Specimens

Post-bonding method have to present same shear strength with only joined and vulcanization usual bush of antiroll bar. Comparing the results, unbonded specimens were tested to obtain shear strength between rubber and steel antiroll bar. The results can be seen in Figure 10. The maximum failure strength was obtained as 4.25 N/mm^2 Experimental results for unbonded specimens were compared with the results of adhesive bonded specimens and then adhesively bonded specimens showed same behavior with the usual vulcanized specimens (Figure 11).

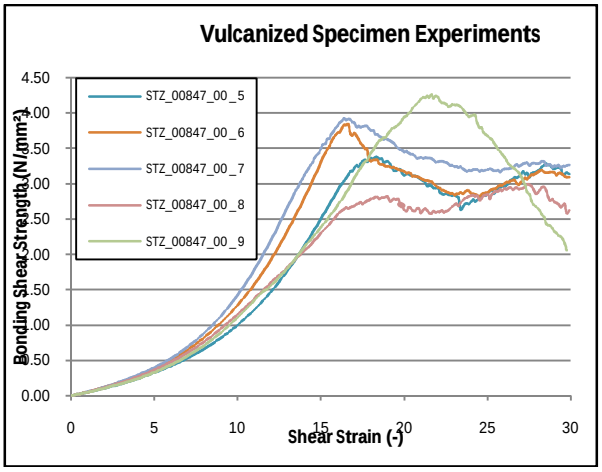

Figure 10: Bonding Test Results of the Vulcanized Bushes

Figure 11: Postmortem Picture of the Bush after Bonding Test

3.4 Difference Between Designed Bushes

Both bushes are mounted in an Ø40 mm diameter casing. In the antiroll bar systems, any sliding between bar and inner surface of bush produces undesirable sounds during vehicle motion. It also causes a temperature ascent due to friction based heat. The latter action affects the life of the rubber bushing as negatively.

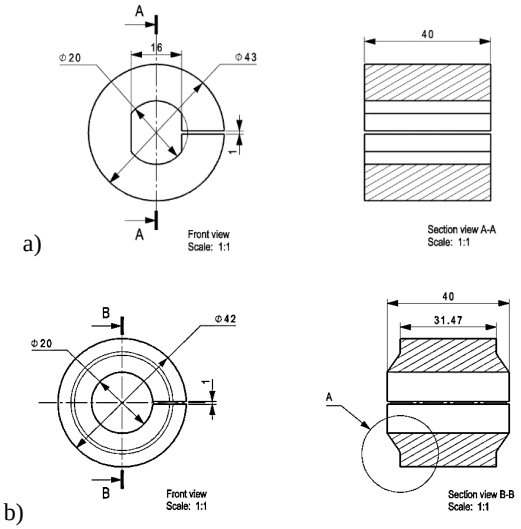

Figure 12:a) Unbonded Mounted Bush b) Adhesively Bonded Mounted Bush

Outer diameter of unbonded specimen was designed bigger than that ofpost-bonded specimens. The outer diameters were Ø43mm and Ø42mm for unbonded and post-bonded specimens respectively. Internal geometryof unbonded specimens also can be seen in Figure 12a such as a slot. Both flattened surfaces give more torque transmitting due to geometrical contact forces. These surfaces have to be machined on the antiroll bar. It also causes additional expenses. But, in post-bonded specimens, this type of machining is not needed on the antiroll bars. Internal geometry of the post-bonded bushes is circular. It can be seen in Figure 12b.Rubber hardness of unbonded bush was measured as 60 ShA and that of post-bonded bush was as 55 ShA. For some much rubber hardness, the unbonded specimen cost is higher than the rubber of the post-bonded specimens.

As for the mounting case, much stress was produced in the unbonded bush, so it required thickened steel sheet brackets and better-quality steels. Those were also impressed in unbonded specimen production costs.

The unbonded specimen weight and post-bonded specimen weight were measured as 55,5gr and 42gr respectively. When it was compared, unbonded specimen was 24,32% heavier than post-bonded specimens.

The post-bonded specimens required one more step as heating in high temperatures in the ovens after vulcanization. This gave a benefit to equalize post-bonded process cost. Moreover, multiple parts can be heated in the oven in one cycle. It can be understood from these inputs that production cost of the post-bonded technique was not higher than the another.

Unbonded specimens were designed in 25% longer time than the post-bonded specimens because of caring for sliding effect. It also increased employee, hardware and software cost.

3.5 Control of Full Vulcanization

In the study, 16 post-bonded bushes were produced by using CAD model given in Figure 11 and according to experimental conditions given in the Table 2. Produced bushes were kept in the oven for adhesive curing. After that the specimens were tested to understand full vulcanization level by radial rigidity experiments. These experiments showed us that described curing time and curing temperature parameters were convenient to complete vulcanization. The experimental results for radial rigidity were given in the Figure 13 and Table 6. The results were verified for full vulcanization due to all radial rigidity results in 15% tolerance.

Table 6: Control of the vulcanization level by radial rigidity experiments

Experiment No	Radial Rigidity (N/mm)	Experiment No	Radial Rigidity (N/mm)
Exp. 1	1396.11	Exp. 09	1308.13
Exp. 2	1384.48	Exp. 10	1320.52
Exp. 3	1381.45	Exp. 11	1496.35
Exp. 4	1395.84	Exp. 12	1501.52
Exp. 5	1370.22	Exp. 13	1582.96
Exp. 6	1337.90	Exp. 14	1426.18
Exp. 7	1486.58	Exp. 15	1384.76
Exp. 8	1347.85	Exp. 16	1464.72

3.6 Bonding Experiments and DoE

Vulcanization level experiments showed that the new post-bonding technique was working as a production process. But, the other important specification was the bonding strength. The results were set to L16 orthogonal array table and demonstrated in Figure 14.

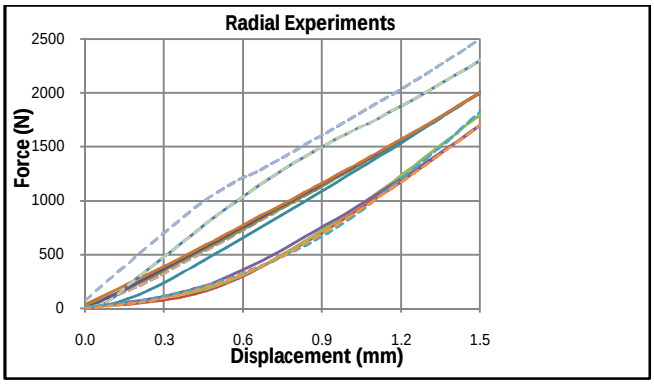

Figure 13: Radial Loading Experiments for Vulcanization Level Control

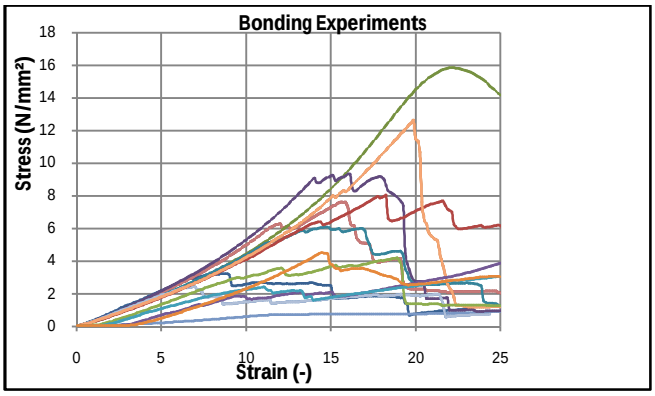

Figure 14: Bonding Experiment Results

After setting bonding experimental results to L16 orthogonal array table, the effects of the factors were analyzed. Calculated effects were sorted out from 1 to 15 and the data were inserted to Normal Probability Graph (NPG) in Figure 14.

The effects of the factors were analyzed in Taguchi method with a central curve. This curve was drawn by using minimum 3 points around the center. The effects of the parameters on the results were evaluated using this curve. According to normal distance comparison, the longest normal distance from the central curve means the highest effective factor.

In the present study, all factors were evaluated to understand the correlation between each other.

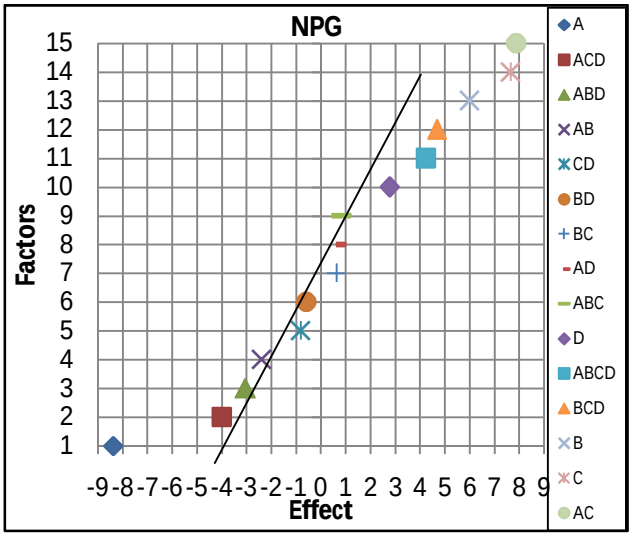

Figure 15: Normal Probability Graph

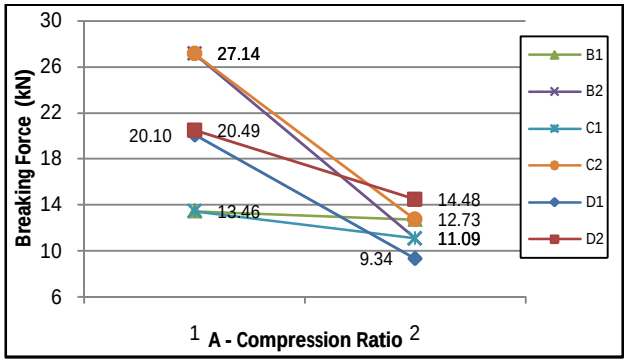

Figure 16: Variation of the B, C, D parameters via A

Table 7: Compression Ratio (A) and Vulcanization Ratio (B) interactions

	B1				B2			
A1	8.00	10.00	18.83	17.00	39.20	23.22	15.05	31.09
	13.46				27.14			
A2	6.07	7.00	19.87	18.00	10.45	13.84	8.85	11.22
	12.73				11.09			

Effects of the factors were obtained by using L16 orthogonal array table. Then the main factors were investigated by a cross mach and included in the tables.

It was seen that there was an interaction between Compression Ratio and Vulcanization Ratio parameters in Table 7 and Figure 16. It can be said that there was no variation in the bonding forces when the vulcanization ratio was 90% and the compression ratio increased from 5% to 10%. If the vulcanization ratio was taken as 80 % and the compression ratio increased from 5% to 10%, in the bonding force a remarkable amount reduction was observed.

Table 8: Interaction between Compression Ratio (A) – Cure Time (C)

	C1				C2			
A1	8.00	10.00	18.83	17.00	39.20	23.22	15.05	31.09
	13.46				27.14			
A2	10.45	13.84	8.85	11.22	6.07	7.00	19.87	18.00
	11.09				12.73			

When the curing time was 2 hours, compression ratio increased from 5% to 10%, the bonding forces decreased in a small amount. If the curing time was 3 hours, compression ratio increased from 5% to 10%, it was observed that there was a significant amount reduction in the bonding forces. Finally, high curing time and low compression ratio were the optimum results in the constant vulcanization ratio and curing temperatures. (Table 8).

Table 9 Interaction between Compression Ratio (A) and Curing Temperature (D)

	D1				D2			
A1	8.00	10.00	39.20	23,22	18.83	17,00	15,05	31.09
	20.10				20.49			
A2	6.07	7.0	10.45	13.84	19.87	18,00	8.85	11.22
	9.34				14.48			

Curing temperatures were fixed at 170°C or 180°C, compression ratio increased from 5% to 10%, the bonding forces in both cases decreased in a remarkable amount. High curing temperature and low compression ratio were the optimum results when the vulcanization ratio and curing time were taken constant (Table 9).

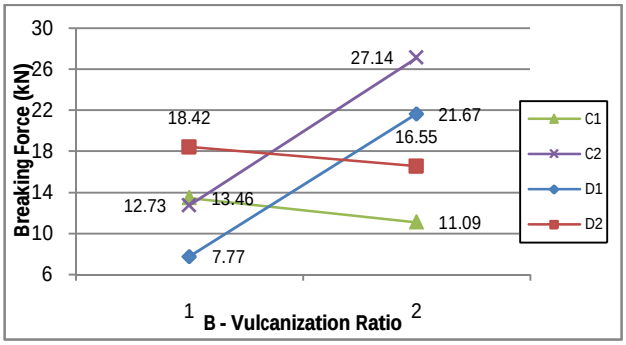

Figure 17: Variation of the C, D Parameters via B

Table 10: Vulcanization Ratio (B) – Cure Time (C) Interaction

	C1				C2			
B1	8.00	10.00	18,83	17,00	6,07	7,00	19,87	18,00
	13.46				12.73			
B2	10.45	13.84	8,85	11,22	39,20	23,22	15,05	31,09
	11.09				27.14			

Figure 17, Table 10 and Table 11 show the interaction between curing time and temperature according to the vulcanization ratio. When the curing time was taken as 2 hours, vulcanization ratio increased from 80% to 90% and the bonding forces increased in a higher slope. If the curing time was taken 3 hours the vulcanization ratio increased from 80% to 90%, a reduction in the bonding force was observed.

Table 11: Interaction between Vulcanization Ratio (B) and Curing Temperature (D)

	D1				D2			
B1	8.00	10.00	6,07	7,00	18,83	17,00	19,87	18,00
	7.77				18.42			
B2	39.20	23.22	10,45	13,84	15,05	31,09	8,85	11,22
	21.67				16.55			

If curing temperature was described constant as 170°C and vulcanization ratio increased from 80% to 90% increased in a higher slope. If the curing temperature was described constant as 180°C and vulcanization ratio increased from 80% to 90%, the bonding force reduced at a very low slope.

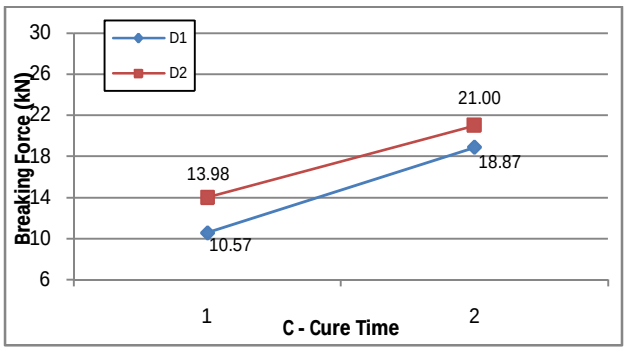

Figure 18: Variation of Parameter C According to D

Table 12: Interaction of Curing Temperature (C) and Curing Time (D)

	D1				D2			
C1	8.00	10.00	10,45	13,84	18,83	17,00	8,85	11,22
	10.57				13.98			
C2	39.20	23.22	6,07	7,00	15,05	31,09	19,87	18,00
	18.87				21.00			

In Figure 18 and Table 12, interactions between the curing Temperature and curing time were given. When curing temperature increased from 170°C to 180°C and curing time increased from 2 hours to 3 hours, bonding forces increased in a very low slope in both cases.

If it was tried to make an optimization between the curing time and the curing temperature and when the vulcanization ratio and the compression ratio were set constant, high curing time and high curing temperature cases gave the results.

It was seen that in the study totally 16 experiments were performed and 8 parameter combinations were investigated. For example, the parameters in experiments 1 and 2 were the same. To eliminate calculation and measurement results, breaking forces were taken as mean values of the two experiments which had the same parameters. An obtained arrangement was shown below as an example according to compression ratio (A1) results.

1) A1, B2, C2, D12) A1, B2, C2, D2
3) A2, B1, C2, D24) A1, B2, C1, D2
5) A2, B2, C1, D16) A2, B2, C1, D2
7) A1, B1, C1, D18) A2, B1, C2, D1

4. CONCLUSION

In the present study, a novel joining technique was studied to solve big metal parts and small rubber bushes contacted with a very small surface. The technique was called a Post-Bonding.

So, in this novel solution, very small vulcanization molds were enough to join the process. The obtained interface forces were equal or more than the common vulcanization techniques values. As a result, this new technique presents superior results in comparison with the usual vulcanization applications.

Four parameters affect the performance of the Post-bonding technique. The most dominant factor was obtained as the compression ratio. But, according to the bonding force level, an optimization of the four parameters presented the best bonding performance in the low compression ratio (A= 5%), high vulcanization ratio (B=90%), high curing time (C= 3 hours) and low curing temperature (D= 170 °C)

The usage the post-bonding technique increases the quality and lifetime of the parts in the vehicle antiroll bar systems.

REFERENCES

1. **FEA in the Design Process of Rubber Bushing**, *ABAQUS Users' Conference*, pp. 1–15, 2002.
2. P.Senapathi, S. Shama, G. Venugopala, B.M. Sachin, S. Krishna, D. Navakishore, Cheryl, Karthikeyan, P.Shripadraj, and R. Basava. **Endurance testing and**

FE analysis of four-wheeler automobile stabilizer bar, *TopTECH SAE and ARAI*, pp. 1-4, Feb. 2009.

3. M.A.Ansarifar, J. Zhang, J. Baker, A. Bell, and R.J. Ellis. **Bonding properties of rubber to steel, aluminium and nylon 6.6.**, *International Journal of Adhesion & Adhesives*, vol. 21, pp. 369–380, 2001.
4. N.A.Darwish, A.B.Shehata, A.I.Abou-Kandil, A.A.Abd El-Megeed, B.K.Saleh, and S.N.Lawandy.**A novel promoter for enhancing adhesion between natural rubber and brass-plated steel cords**, *International Journal of Adhesion & Adhesives*, vol.40, pp. 135–144, 2013.
5. A.Souid, A.Sarda, R.Deterre, and E. Leroy.**Test method influence of reversion on adhesion in the rubber-to-metal vulcanization-bonding process**, *Polymer Testing*, vol. 41, pp. 157–162, 2015.
6. A.D.M. Africa, M.L.B. Esteban, and H.M. Orines. **Vehicular Speed Limiting Control System in Critical Zones Using Global Positioning System**, *International Journal of Emerging Trends in Engineering Research*, vol. 8. no. 5, pp. 859-863, 2020.https://doi.org/10.30534/ijeter/2020/72852020
7. S. Mothe, A.S. Teja, B. Kakumanu, and R.K. Tata.**A Model for Assessing the Nature of Car Crashes using Convolutional Neural Networks**, *International Journal of Emerging Trends in Engineering Research*, vol. 8. no. 3, pp. 2173-2176, 2020. https://doi.org/10.30534/ijeter/2020/41832020
8. E. Julianto, M. Effendy, and Gunarto.**Application of Float Glass for Car Windshield,***International Journal of Emerging Trends in Engineering Research*, vol. 8. no. 5, pp. 2173-2176, 2020. https://doi.org/10.30534/ijeter/2020/11285202
9. T.Ansys, P.M.Bora, and P.K.Sharma.**Vehicle Anti-Roll Bar Analyzed Using FEA**, *International Journal of Advanced Technology in Engineering and Science*, vol. 2, issue 7, pp. 130–136, July 2014.
10. A.T.Kanaev, G.K.Taimanova, and T.E. Sarsenbaeva.**Differential Head Treatment of One-Piece Freight-Car Wheels**, *Steel*, vol. 47, no. 5, pp. 345–348, 2017.
11. M.V.Blundell.**The influence of rubber bush compliance on vehicle suspension movement**, *Materials and Design*, vol. 19, pp. 29–37, 1998.
12. J. Marzbanradand A.Yadollah.**Fatigue life of a passenger car**, *International Journal of Mechanical and Mechatronics Engineering*, vol. 6, no: 2, pp. 407–413, 2012.
13. P.H. Cronje and P.S.Els.**Improving off-road vehicle handling using an active anti-roll bar,***Journal of Terramechanics*, vol. 47, pp. 179–189, 2010.
14. A. Tarhini and R.F.Hamade.**Numerical simulations of the cathodic delamination of adhesive bonded rubber/steel joints**, *International Journal of Adhesion & Adhesives*,vol. 35, pp. 108–113, 2012.
15. Z.Y.Ren, Q.S.Chen, H.B.Bai, and Y.W.Wu.**Study on damping energy dissipation characteristics of cylindrical metal rubber in nonforming direction**, *Ann. Mater. Sci. Eng*, pp. 1–10, 2018.
16. P.Yang, H.B.Bai, X.Xue, K.Xiao, and X.Zhao.**Vibration reliability characterization and damping capability of annular periodic metal rubber in the non-molding direction**, *Mech. Syst. Signal Process*, vol. 132, pp. 622–639, 2019.
17. B.Harshal, K.Rushikesh, and P.Baskar.**Finite Element Analysis of Anti-Roll Bar to Optimize the Stiffness of the Anti-Roll Bar**, *International Journal of Modern Engineering Research*, May, pp. 11–23, 2014.
18. M.Nakache, E.Aragon, L.Belec, F.X.Perrina, G.Roux, and P.Y.Le Gac.**Degradation of rubber to metals bonds during its cathodic delamination, validation of an artificial ageing test**, *Progress in Organic Coatings*, vol. 72(3), pp. 279–286, 2011.
19. A.N.Khartode and Prof. U. Gaikwad Mahendrals.**Design and Analysis of Antiroll Bars for Automotive Application**, *International Journal on Recent and Innovation Trends in Computing and Communication*,vol. 4, issue 6, pp. 340 – 345, June 2016.
20. T.M.Mohammad, S.M.Sapuan, M.R.Mansor, and A.N.Abdul. **Development of an Automotive Anti-Roll Bar: A Review**, *Journal of the Society of Automotive Engineers Malaysia*, vol. 1, issue 1, pp. 63-81, January 2017.
21. M.T.Mastura, S.M.Sapuan, M.R.Mansor, and A.A.Nuraini.**Conceptual design of a natural fibre-reinforced composite automotive anti-roll bar using a hybrid approach**, *Springer-Verlag London*, pp. 2031-2048, 2016.
22. H.Bayrakceken, S.Tasgetiren, and K.Aslantas.**Fracture of an automobile anti-roll bar**, *ELSEVIER*,vol. 6, pp. 732–738, September 2005.
23. G.E.Tupholme.**An analogy between radially-loaded rubber bush mountings and axially-loaded bonded rubber blocks**, *Materials and Design*,vol. 32, pp. 5038–5042, 2011.
24. J.M.Horton and G.E.Tupholme.**Approximate radial stiffness of rubber bush mountings**, *Materials and Design*,vol. 27, pp. 226–229, 2006.
25. R.Iraj, P.Zahedi, and A. Rezaeian.**Rubber Adhesion to Different Substrates and Its Importance in Industrial Applications: A Review**, *Journal of Adhesion Science and Technology*, vol. 26, pp. 721–744, 2012.
26. X.Wang, W.Xu, Y.Huang, M.Zhong, and H. Fan.**Simulation of The Vertical Bending Fatigue Test of a Five-Link Rear Axle Housing**, *International Journal of Automotive Technology*, vol. 13, no. 6, pp. 923-932, 2012.
27. S.Kayaci, M.Cevher, and Y.E.Eşiyok.**Experimental investigation on the dynamic modulus change of Natural Rubber under principal loading modes and different dynamic conditions**, in*MSC User Conference*, Istanbul, 2011, pp. 1-13.
28. A.K.Serbest, M.Yazici, and A.Bayram.**Interrupted Curing Application for Adhesion of the Vehicle Steel Antiroll Bar and Rubber Bushings**, in*OTEKON'14 7th Automotive Technologies Congress* 24-26 May, Bursa, 2014, pp. 1-11.